

LA-UR- 02-5688

Approved for public release;
distribution is unlimited.

Title: VIBRATION MODELING AND SUPPRESSION
IN TENNIS RACQUETS (u)

Author(s): Miles A. Buechler, LANL, LADSS Program, (MSU)
Luis A. Espino, LANL, LADSS Program, (UT, El Paso)
Gordon A. Thompson, LANL, LADSS Program, (RH)
Rachel Shinn, LANL, LADSS Mentor, (ERAU)
Charles Farrar, LANL, ESA-WR, LADSS Instructor

Submitted to: IMAC Conference
Orlando-Kissimmee, Florida
February 3-6, 2003



Los Alamos National Laboratory, an affirmative action/equal opportunity employer, is operated by the University of California for the U.S. Department of Energy under contract W-7405-ENG-36. By acceptance of this article, the publisher recognizes that the U.S. Government retains a nonexclusive, royalty-free license to publish or reproduce the published form of this contribution, or to allow others to do so, for U.S. Government purposes. Los Alamos National Laboratory requests that the publisher identify this article as work performed under the auspices of the U.S. Department of Energy. Los Alamos National Laboratory strongly supports academic freedom and a researcher's right to publish; as an institution, however, the Laboratory does not endorse the viewpoint of a publication or guarantee its technical correctness.

Form 836 (8/00)

VIBRATION MODELING AND SUPPRESSION IN TENNIS RACQUETS

Miles A. Buechler¹, Luis A. Espino², Gordon A. Thompson³, Rachel Shinn⁴

¹ Dept. of Mechanical Engineering, Montana State University, Bozeman, MN, 59717

² Dept. of Civil Engineering, The University of Texas at El Paso, El Paso, TX, 79968

³ Dept. of Mechanical Engineering, Rose-Hulman Inst. of Technology, Terre Haute, IN, 47803

⁴ Embry-Riddle Aeronautical University, Mentor.

ABSTRACT

The size of the "sweet spot" is one measure of tennis racquet performance. In terms of vibration, the sweet spot is determined by the placement of nodal lines across the racquet head. In this study, the vibrational characteristics of a tennis racquet are explored to discover the size and location of the sweet spot. A numerical model of the racquet is developed using finite element analysis and the model is verified using the results from an experimental modal analysis. The effects of string tension on the racquet's sweet spot and mode shapes are then quantified. An investigation is also carried out to determine how add-on vibrational dampers affect the sweet spot.

NOMENCLATURE

T_{pq}	Transmissibility of output point p with respect to input point q
H_{pq}	Frequency Response Function of impact at point p received at point q
H_{qq}	Frequency Response Function of drive point
$[V]$	i^{th} eigenvector from experimental data
$[V]$	j^{th} eigenvector from numerical solution
$[H]$	Frequency Response Function matrix
ω	Frequency
ϕ	Eigenvector normalized to unit modal mass
λ	Diagonal matrix of natural frequencies
I	Identity Matrix
$F(\omega)$	Fourier transform of forcing function

1 INTRODUCTION

Tennis players have always sought the perfect tennis racquet. Tennis players often refer to a point or area in

the racquet called the "sweet spot". In terms of performance, the sweet spot plays an important role in tennis racquet design. Since the early 1970s, tennis racquets have been designed to increase or expand the area of the sweet spot in an effort to transmit less vibration to the tennis player's hand. This task has kept tennis racquet manufacturers busy for nearly three decades.

According to tennis players, the "sweet spot" is where, when the ball is hit in that point or area, minimal vibration is transmitted to the player's hand and forearm and, as a consequence, the player is almost unaware that the impact has occurred. Although the sweet spot's definition is based primarily on tennis players' experience, several studies have shown that the sweet spot can be related to three different physical phenomena [1] [2] [3]. Each phenomenon is associated with a different location on the racquet. The first racquet point related to the sweet spot is the center of percussion. The center of percussion of a tennis racquet is the point where the translational and rotational forces cancel each other, resulting in minimal sensation of hitting the ball [3]. The second location of the sweet spot corresponds to the maximum coefficient of restitution on the racquet head. The point of the maximum coefficient of restitution is where the ball, if released in free fall towards the racquet head, would have the maximum rebound. Hitting the ball with this spot will provide the ball with more rebound than any other spot on the racquet head. The third point on the racquet associated with the sweet spot is related to the concept of nodal lines across the racquet head. The nodal lines are the lines or zones of zero displacement in the mode shapes when the racquet is excited. When the racquet is hit on a point along these nodal lines, the racquet, theoretically, would not experience any vibration from that mode and, consequently, the player would not feel any impact or vibration on his hand. By this definition, the sweet spot occurs at the crossing of several nodal lines on the racquet face.

This paper explores and analyzes the vibration characteristics of a tennis racquet. A tennis racquet was tested by hitting every other string intersection as well as selected points on the racquet frame. The response accelerations caused by each hit were measured for trials with and without commercial damper suppression devices. Using commercial experimental modal analysis software, ME'scope™, modal analysis was performed in order to identify the mode shapes of the racquet. A commercial finite element code, ABAQUS/CAE™, was used to model the structure of the tennis racquet. The finite element model was refined to match the mode shapes and frequencies identified previously from the experimental results. Finally, a transmissibility study was performed in order to investigate the real effects of the vibration suppression devices on the tennis racquet.

2 EXPERIMENTAL PROCESS

The purpose of the experiment was to identify the different mode shapes and natural frequencies of the racquet and to discover the impact that different kinds of dampers have on the racquet's vibrational characteristics. To do this, the tennis racquet was subjected to roving impact testing, hitting the frame and every other string intersection while the accelerations of the tennis racquet frame were recorded at three fixed locations.

2.1 Test Racquet Description

The racquet tested was a Junior JR-10™ model made of a hollow aluminum frame and nylon monofilament strings. The frame has a constant cross-section but varying curvature. The vertical strings were not evenly spaced; rather, they were closer together in the middle of the racquet. The distances between horizontal strings were approximately the same. The racquet measured 60.9-cm (24-in.) from the top of the head to the bottom point of the handle. The head of the racquet was 25.7-cm-wide (10.1-in-wide) and the handle measured 14.3-cm (5.62-in) long, 3.15-cm (1.25-in) wide, and 3-cm (1.18-in) depth. Figure 1 shows the racquet with its dimensions. The racquet tested was a used racquet, so the string tension was much lower than the 200-267 N (45-60 lbf) typical for a new racquet. The actual string tension was estimated to be 31-36 N (7-8 lbf).

2.2 Vibration Suppression Devices Description

In order to determine the effect of vibration suppression devices, two different commercial dampers, shown in Figure 2, were used to test the racquet. Damper 1 and Damper 2 were placed between the lower strings of the racquet. Figure 1 shows the position of the commercial dampers.

2.3 Test Setup/Data Acquisition

Free-free boundary conditions are a good model for a player gripping the handle, because the natural frequencies for both cases are very similar [1]. For experimental testing, the racquet was suspended by the

handle using an approximately 1 meter-long elastic cord in order to simulate free-free boundary conditions around the racquet as shown in Figure 3. Measurements were taken normal to the plane of the racquet at selected points on the strings, frame, and handle.

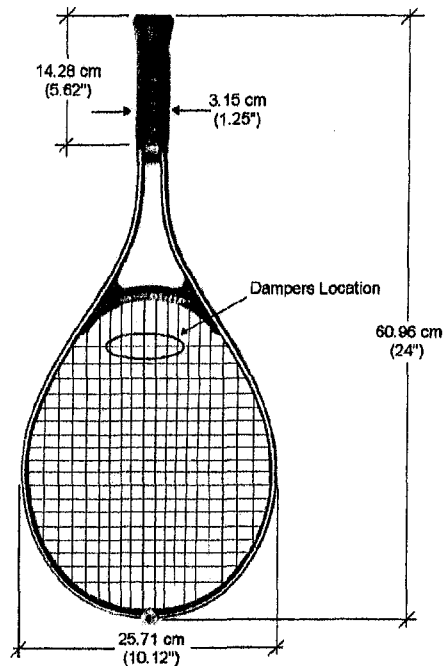


Figure 1. Racquet model dimensions

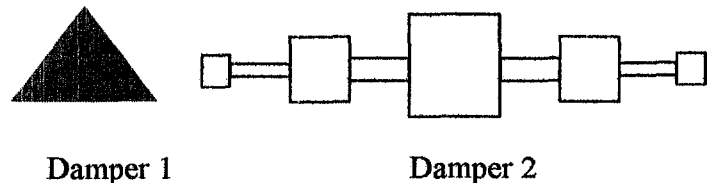


Figure 2. Vibration suppression devices

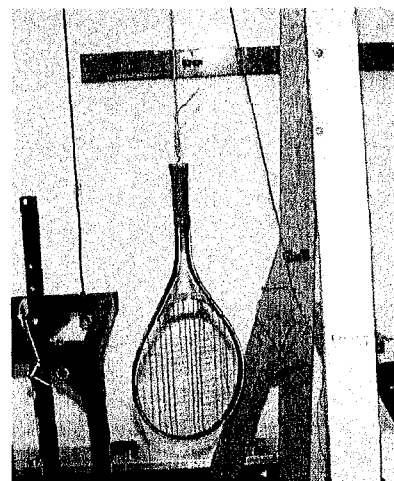


Figure 3. Racquet test configuration

The tennis racquet was instrumented with 3 PCB Piezotronics® 352C22 accelerometers. The nominal sensitivity and range of the accelerometers were 10mV/g and \pm 500 g respectively. The accelerometers were placed with wax at different locations on the tennis racquet frame (See Figure 4). Placing an accelerometer on the strings decreased the natural frequency of the string modes by 8%. Consequently, accelerometers were placed solely on the frame to prevent these effects on the strings. Unfortunately, this placement made accurate estimates of several string modes difficult, because their nodes lay along the frame. A PCB Piezotronics® 086D80 impact hammer was used to excite the tennis racquet. The force transducer on the impact hammer had a range of 0-222 N (0-50 lbf) and nominal sensitivity of 2.25 mV/N (100mV/lbf).

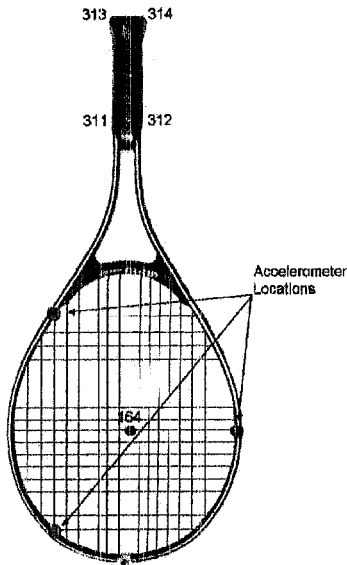


Figure 4. Accelerometer locations

Force and acceleration data were collected by means of a Dactron four-channel Photon™ Dynamic Signal Analyzer analysis data acquisition system using Dactron's RT Pro™ Signal Analysis and Waveform software controlled from a Dell laptop PC. Data were recorded for 1.364 seconds at a rate of 2048 points per sample, corresponding a frequency of 600 Hz. A Force/Exponential window was applied to these measurements. Five runs were averaged to calculate the racquet frequency response functions (FRF's). The FRF's were exported in ASCII Universal File Format for analysis in ME'scope™ modal analysis software. ME'scope™ was used to extract the modal parameters of frequency, damping, and shape.

2.4 Test Variations

During preliminary testing, the natural frequencies of the racquet's string modes varied by as much as 8% from day to day. The most likely cause of these variations was a change in the ambient temperature and humidity, causing changes to the string tension. Experiments were

conducted in a room without climate control, resulting in day-to-day environmental variations. Another cause for variations could be shifts in the racquet strings, resulting in a slightly different racquet shape.

In order to reduce the effects of the frequency shifts, each test was completed in a single sitting. When testing the racquet with the vibration dampers, a single measurement was taken without a vibration damper attached, to calibrate the random frequency shifts.

2.5 Test Results

Because the tests were conducted on different days, the natural frequencies of the undamped racquet varied between tests. By comparing the calibration FRF's from the damper tests with the FRF's from the undamped racquet test, it was shown that the natural frequencies of the undamped racquet varied by as much as 2.3% for this test data. These shifts only affected modes associated with the racquet strings. Modes confined to the frame were unaffected by frequency shifts.

The experimental data were imported into ME'scope™ in order to estimate mode shapes and natural frequencies. ME'scope™ uses parametric curve fit estimation, in this case a single reference global polynomial method, to find mode shapes and natural frequencies from the FRF's. Once mode shapes and natural frequencies have been found, ME'scope™ animates the resulting deformations of the structure.

The addition of dampers changed the mode shapes of the racquet significantly. A summary of the natural frequencies and percent critical damping for the undamped racquet can be seen in Table 1. Table 2 shows the natural frequencies and percent critical damping for the racquet when damped with Damper 1. Table 3 shows the results for the racquet when damped with Damper 2.

Frequency (Hz)	% Critical Damping	Mode
130	1.17	Frame Bending
246	0.368	String Percussion
303	0.653	Frame Torsion
316	1.31	Saddle
387	0.277	
398	0.334	
489	1.12	2nd Frame Torsion
492	0.218	
524	0.289	
536	0.31	
575	0.323	

Frequency (Hz)	% Critical Damping	Mode
126	2.51	Frame Bending
195	0.654	Damper Percussion
265	0.447	String Percussion
307	1.83	Frame Torsion
312	1.29	Saddle
394	0.43	
408	0.483	
437	1.12	
484	0.773	2nd Frame Torsion
508	1.00	
530	—	
543	0.456	
571	0.623	
596	0.612	

Frequency (Hz)	% Critical Damping	Mode
127	1.51	Frame Bending
195	0.601	Damper Percussion
269	0.43	String Percussion
286	0.727	Damper Torsion
306	0.701	Frame Torsion
313	1.27	Saddle
354	0.823	
397	0.819	
419	0.69	
436	0.347	
483	0.703	2nd Frame Torsion
559	0.285	
565	0.321	
607	0.282	

3 FINITE ELEMENT ANALYSIS

A finite element (FE) model of the tennis racquet was developed in order to simulate the effects of increased string tension on the mode shapes and frequencies. The finite element analysis was performed using the ABAQUS/CAE™. The frame and strings were modeled using beam elements. The string nodes were coupled, making the string intersections solid connections instead of friction joints. The model was refined to match the results from the tennis racquet with no damper on it. Having achieved the desired results for the FE model, the commercial vibration dampers were modeled and added in

between the bottom strings of the existing racquet model. Finally, the string tension was increased.

4 ANALYSIS OF RESULTS

4.1 Experimental Modal Analysis

The addition of dampers to the tennis racquet changed the experimental natural frequencies and mode shapes of the string modes but had almost no effect on the frame modes.

Undamped Racquet

Modal analysis of the undamped racquet revealed 11 modes within the first 600 Hz. These modes included both modes confined to the frame and modes confined to the strings. Frame modes had a higher percent critical damping (0.653%-1.31%) than string modes (0.218%-0.368%). This difference in damping can be explained by the difference in materials, aluminum for the frame and nylon for the strings.

Damper 1

The addition of Damper 1 to the tennis racquet resulted in notable changes to the string modes of the system. It increased the frequency of the modes by as much as 7.7%. The damper had no effect on the frame modes of the racquet. Furthermore, the damping of the system was insensitive to the damper. This results indicates that the device is not a true vibration damper per se, but rather a vibration suppressor.

Damper 1 split the first string percussion mode of the undamped system, located at 246 Hz, into two modes surrounding the undamped percussion mode. The first, a damper percussion mode located at 195 Hz, involves motion of the dampers and nearby strings. The second is a lower intensity string percussion mode, located at 265 Hz. The damper also changed the shapes of the higher frequency modes, as well as adding several new modes.

Damper 2

Like Damper 1, Damper 2 had a significant effect upon the natural frequencies and mode shapes of the string modes. The damper changed the string mode shapes to the extent that comparing modes is almost impossible. For example, the undamped racquet has a string mode at 387 Hz. Similar mode shapes appear twice in the racquet with Damper 2, at 354 Hz and 436 Hz. The damper had no effect on the frame modes or the critical damping of the system.

Damper 2 also split the first string mode of the undamped racquet into two lesser modes. The first, again a damper percussion mode, is located at 195 Hz. The second, a reduced string percussion mode, is located at 269 Hz. Damper 2 had a greater effect on the higher frequency mode shapes than Damper 1. For Damper 1, seven modes can be correlated with the undamped mode

shapes. For Damper 2, however, only six mode shapes can be correlated.

4.2 Transmissibility

Although the changes in mode shapes show some of the effects of the vibration dampers, a more useful and quantitative comparison involves the transmission of vibrations through the racquet. Commercial vibration dampers are marketed as reducing harmful vibrations, which cause tennis elbow. The obvious question, then, is whether they really reduce vibrations? As a partial answer to this question, the transmissions of vibrations from an impact on the sweet spot to several points on the handle of the racquet have been calculated. These points, numbers 311, 312, 313, and 314, can be seen in Figure 4.

The transmissibility of vibrations, T_{pq} , is calculated by the following equation:

$$T_{pq} = \frac{H_{pq}}{H_{qq}} \quad (1)$$

where H_{pq} is the FRF for striking the racquet at the handle and receiving at the sweet spot and H_{qq} is the FRF for the drive point measurement at the sweet spot.

The vibration dampers do have an effect on the transmissibility from the sweet spot to the handle, as can be seen in Figure 5. In general, they reduce higher frequency vibrations, but they increase vibrations at lower frequencies. Both dampers reduce a peak at 530 Hz. This peak is reduced from almost 15% transmissibility in the undamped racquet to 2% transmissibility for Damper 1 and no transmissibility for Damper 2. This reduction in vibrations comes at a price, though. Both dampers increase the transmissibility between 180 Hz and 330 Hz. The undamped racquet transmits 8% of the vibrations at 320 Hz. The racquet with both dampers transmits more; Damper 1 has transmissibility near 15% and Damper 2 has a transmissibility of 10%. In addition, both dampers have several other peaks between 180 Hz and 330 Hz, while the undamped racquet has none.

The transmissibilities of the damped systems have fairly large uncertainties associated with them. These uncertainties come from the fact that several string modes have nodes located on the frame where the accelerometers were attached. As a result, the magnitude of these modes is unclear when curve fitting. By choosing different damper magnitudes, the transmissibility of Damper 1 and Damper 2 vary between 10% and 25% in the 180 Hz to 330 Hz range. Although the actual value of the transmissibility is uncertain, it is definitely higher than the undamped transmissibility.

4.3 Correlation of FE model

The Modal Assurance Criteria (MAC) was used to characterize the similarity between the FE model and the experimental results.

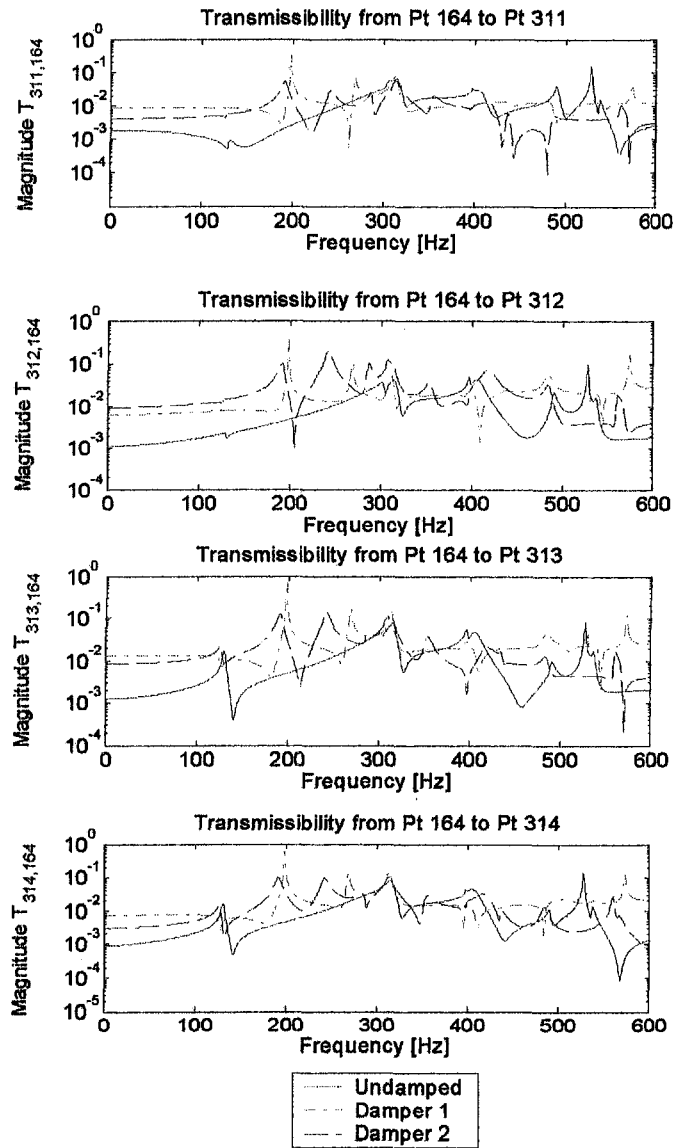


Figure 5. Transmissibility of points on racquet handle.

$MAC_{i,j}$, indicating the similarity between the i^{th} eigenvector of the experimental data and the numerically determined j^{th} eigenvector is calculated using the following equation:

$$MAC_{i,j} = \frac{|[V_i]^* \cdot [V_j]|^2}{([V_i]^* \cdot [V_i])([V_j]^* \cdot [V_j])} \quad (2)$$

where V_i indicates the eigenvector of the i^{th} mode of the experimental system, and the V_j components indicate the numerically calculated eigenvectors. A correlation coefficient of 1 indicates that the experimental and numerically determined modes are the same. Conversely, a coefficient approaching 0 indicates no correlation. An

ideal MAC is a square identity matrix. This would indicate excellent correlation of each FE mode with the corresponding experimentally determined mode, as well as no correlation between modes of different designations.

The first step in applying the MAC was to reduce the FE output of all the degrees of freedom to the points at which experimental data were collected. The reduction was performed using a MATLAB script.

Figure 6 is a 3-D bar plot of the MAC for the undamped model. A correlation coefficient of greater than 0.95 was achieved with the undamped model for modes 1, 2, 5, and 6. Mode switching, a common phenomenon when modeling real structures, occurred for modes 3 and 4 as well as 7 and 8. There were several coefficients above 0.7, which would ideally have been 0. This was possibly due to the assumptions made in modeling the string crossings.

Similar results were obtained for both damped models.

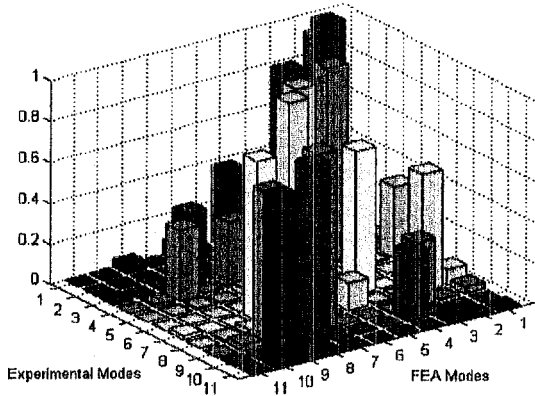


Figure 6. Correlation of Undamped model

4.4 Simulation of higher Tension

The string tension of the actual racquet was qualitatively observed to be lower than that of an unused racquet. This observation is supported through the correlation of the numerical model, which used a string tension of less than 24 N. A numerical analysis was performed to determine the effect of string tension on the frequencies and shape of each mode. Correlation was calculated for each of the modes and a correlation of greater than 0.9 was chosen as the criteria for mode shape similarity. The difference in frequency for similar mode shapes was divided by the frequency of the low-tension mode to determine the frequency shift. As shown in Tables 4 through 6, frame modes were relatively unaffected by changes in string tension; however, the frequency of string modes, such as the first percussion mode, were increased.

Table 4. Effect on modal frequencies of string tension of undamped model.

23 N	100 N	Correlation	Frequency Shift
1*	1*	0.996	-1.08%
2	4	0.975	84.5%
3*	2*	0.949	-3.08%
4*	3*	0.974	-3.48%
5	9	0.994	93.1%
6	8	0.998	89.1%
8	11	0.997	89.3%
9	12	0.93	84.6%
10	13	0.995	88.5%

* indicates frame modes

Table 5. Effect of string tension on modal frequencies of model damped with Damper 1.

23 N	100 N	Correlation	Frequency Shift
1*	1*	0.986	0.86%
3	4	0.917	78.3%
5*	3*	0.973	-3.48%
6	8	0.996	89.7%
7	9	0.987	89.2%

* indicates frame modes

Table 6. Effect of string tension on modal frequencies on model damped with Damper 2.

23 N	100 N	Correlation	Frequency Shift
1*	1*	0.964	0.32%
2	4	0.95	74.9%
3	5	0.987	87.5%
4	6	0.907	85.9%
7	11	0.997	66.2%
8	13	0.926	68.0%

* indicates frame modes

The numerical model was also used to gain an understanding of how string tension affects the transmissibility of vibrations to the handle. Transmissibility was calculated using Equation 1; however, the [H] terms were calculated numerically as:

$$[H(\omega)] = \{\phi\} [\lambda - \omega^2 I]^{-1} \{\phi\}^T \{F(\omega)\} \quad (3)$$

where $[\phi]$ is the eigenvectors normalized to unit modal mass, and $[\lambda]$ is the diagonal natural frequency matrix both of which were exported from ABAQUS after a frequency extraction load step. ω was an equally distributed 810 element vector created from 0-650 Hz.

$F(\omega)$ was the Fourier transform of $\cos(\omega t)$ applied only at the node corresponding to point 164, at the center of the racquet face. The rest of the matrix were zeros. H_{pq}

is the p^{th} row of the H matrix, and H_{qq} is the q^{th} row.

This model neglected internal damping, so the magnitude of the numerically calculated transmissibility doesn't correspond well with the experimental results, but trends were analyzed qualitatively.

Like the string mode shapes, the increased transmissibility peaks occurred at higher frequencies when greater string tension was modeled. As can be seen in Figure 7, the numerical analysis of the add-on dampers concurs with the experimental data in that the transmissibility peaks decrease in frequency after addition of either damper. Unlike the experimental results, the numerical model predicted a transmissibility decrease of about 70% when Damper 1 was applied to the loose string racquet model.

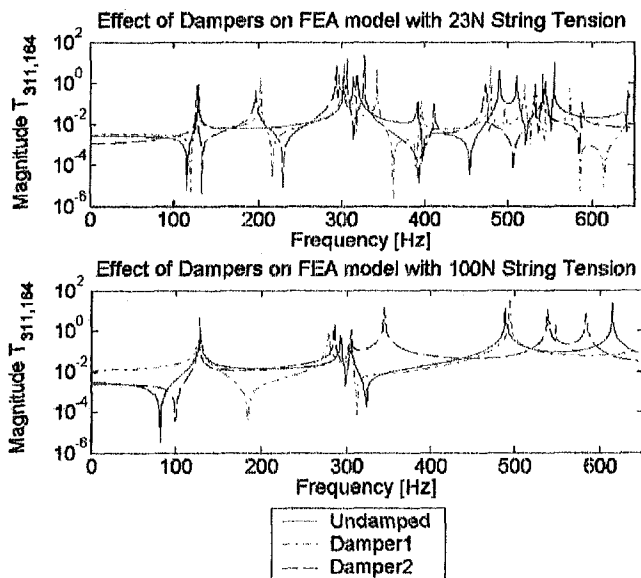


Figure 7. Numerically calculated transmissibility for 23 N and 100 N.

5 CONCLUSIONS

Using the nodal lines definition of the sweet spot, the location of the sweet spot is located at the anti-node of the first string percussion mode. This anti-node is also very close to the node of the first frame bending mode. Consequently, most of the energy goes into the strings and is then returned to the ball. In addition, because the frame is not excited, the player feels few vibrations at the handle.

The commercial vibration dampers were seen to have a varied influence on vibrations at the handle. Although they damp out vibrations near 500 Hz, they cause more vibrations to be transmitted between 180 Hz and 330 Hz. This result holds true for the experimental racquet as well as the FE model of higher string tension.

Using the FE model for higher string tension, the string mode shapes do not change. The frequencies they occur at increase by almost 90%, but the shapes themselves stay the same.

ACKNOWLEDGEMENTS

This research project was completed at Los Alamos National Laboratory as part of The Third Los Alamos Dynamics Summer School. Funding for the Los Alamos Dynamics Summer School was provided by the Engineering Science and Applications Division at the Los Alamos National Laboratory and the Dept. of Energy's Education Programs Office. The following companies generously provided various software packages that were necessary to complete the student projects: Vibrant Technologies (experimental modal analysis software), The Mathworks, Inc. (numerical analysis software), and Hibbitt, Karlsson and Sorensen, Inc. (ABAQUS finite element software). The authors would like to thank Rachel Shinn for mentoring our group and Chuck Farrar the director of Los Alamos Dynamics Summer School program.

REFERENCES

- [1] Brody, H., (1995) "How would a physicist design a tennis racket?" Journal of Physics today, pp. 26-31
- [2] <http://www.racquetresearch.com>
- [3] http://www.mittusa.com/technical/technical_information